Journal of Translational Medicine

RESEARCH

Open Access

Circadian rhythm disruption modulates enteric neural precursor cells differentiation leading to gastrointestinal motility dysfunction via the NR1D1/NF-κB axis

Yurui Zhang[1], Shizhao Xu[1], Mengke Fan[1], Hailing Yao[1], Chen Jiang[1], Qi He[1], Huiying Shi[1*] and Rong Lin[1*]

Abstract

Objectives Circadian rhythm disruption (CRD) is implicated with numerous gastrointestinal motility diseases, with the enteric nervous system (ENS) taking main responsibility for the coordination of gastrointestinal motility. The purpose of this study is to explore the role of circadian rhythms in ENS remodeling and to further elucidate the underlying mechanisms.

Methods First, we established a jet-lagged mice model by advancing the light/dark phase shift by six hours every three days for eight weeks. Subsequent changes in gastrointestinal motility and the ENS were then assessed. Additionally, a triple-transgenic mouse strain (Nestin-creER^{T2} × Ngfr-DreER^{T2}: DTRGFP) was utilized to track the effects of CRD on the differentiation of enteric neural precursor cells (ENPCs). RNA sequencing was also performed to elucidate the underlying mechanism.

Results Compared to the control group, CRD significantly accelerated gastrointestinal motility, evidenced by faster intestinal peristalsis ($P < 0.01$), increased fecal output ($P < 0.01$), and elevated fecal water content ($P < 0.05$), as well as enhanced electrical field stimulation induced contractions ($P < 0.05$). These effects were associated with an increase in the number of glial cells and nitrergic neurons in the colonic myenteric plexus. Additionally, ENPCs in the colon showed a heightened differentiation into glial cells and nitrergic neurons. Notably, the NR1D1/nuclear factor-kappaB (NF-κB) axis played a crucial role in the CRD-mediated changes in ENPCs differentiation. Supplementation with NR1D1 agonist or NF-κB antagonist was able to restore gastrointestinal motility and normalize the ENS in jet-lagged mice.

Conclusions CRD regulates the differentiation of ENPCs through the NR1D1/NF-κB axis, resulting in dysfunction of the ENS and impaired gastrointestinal motility in mice.

Keywords Circadian rhythm, NF-κB signaling, Enteric nervous system, Enteric neural precursor cells, Gastrointestinal motility

*Correspondence:
Huiying Shi
shihuiying23@hotmail.com
Rong Lin
linrong@hust.edu.cn
[1]Department of Gastroenterology, Union Hospital, Tongji Medical College, Huazhong University of Science and Technology, Wuhan 430022, China

Introduction

Circadian rhythms are 24-hour patterns generated by molecular clocks, which synchronize the biological functions of organisms with the external environment cues [1]. These rhythms can be disrupted by various factors such as artificial light, mistimed eating, and irregular physical activity [2]. In modern society, circadian rhythm disruption (CRD) due to conditions like jet lag and shift work has become increasingly prevalent, particularly in professions where such disruptions are unavoidable [3]. This disruption has led to numerous adverse health outcomes, making CRD a growing global health concern [4, 5].

Gastrointestinal function exhibits circadian rhythms across various processes, including gastric acid secretion, gastric emptying, digestive enzyme production, and intestinal motility [6]. CRD has been associated with an increased prevalence of functional gastrointestinal disorders. Clinical studies have demonstrated that shift workers are at a higher risk of developing such disorders, including irritable bowel syndrome (IBS), gastroesophageal reflux disease (GERD), and functional dyspepsia, compared to individuals with traditional daytime work schedules [7–9]. Nojkov et al. reported a significantly higher prevalence of abdominal pain among nurses working rotating shifts compared to those on fixed day or night shifts [8]. Similarly, Chen et al. observed a positive correlation between shift work and GERD, with a higher prevalence of GERD among night and shift workers compared to non-shift workers [9]. Collectively, these findings suggest that CRD may play a critical role in the development and progression of gastrointestinal dysfunction. However, the precise mechanisms through which CRD leads to gastrointestinal dysfunction remain insufficiently explored.

The enteric nervous system (ENS), composed of a complex network of neurons and glial cells, is a crucial autonomic nervous system located in the gastrointestinal wall. This system includes intrinsic primary afferent neurons, interneurons, and motor neurons, each distinguished by specific neurochemical coding and function [10]. These neurons are organized into two interconnected networks: the myenteric and submucosal plexuses [11]. The myenteric plexus primarily regulates the muscular contractions responsible for propelling gut contents, while the submucosal plexus governs secretion and absorption processes [12]. The ENS exhibits significant functional and structural plasticity, including alterations in the properties of enteric glial cells and neurons, which play a crucial role in the development of gastrointestinal dysfunction [13]. For example, a significant reduction in enteric neurons, particularly inhibitory neurons, in the lower esophagus may contribute to the development of achalasia. This reduction impairs esophageal peristalsis and prevents the lower esophageal sphincter from relaxing during swallowing [14]. In cases of slow-transit constipation, there is a marked decrease in both the size and number of enteric ganglia, as well as a reduction in the quantity of enteric glial cells and neurons [11]. Previous studies have shown that the transcriptional activity of the ENS undergoes significant changes due to circadian rhythms [15]. However, little is known about whether CRD can induce structural and functional changes in the ENS, as well as the role such changes may play in gastrointestinal dysfunction.

Even under physiological conditions, the shape of the ENS is altered by mechanical deformations resulting from the contraction and relaxation of the intestinal wall muscles [10]. These mechanical stresses cause significant apoptosis of enteric neurons, which is offset by a comparable level of neurogenesis, thereby preserving the overall integrity of the ENS throughout its lifespan. Enteric neural precursor cells (ENPCs), derived from the neural crest stem cells of the gut, primarily express nerve growth factor receptor (Ngfr) and Nestin [16]. These cells have the capacity for self-renewal and differentiation into enteric neurons and glial cells, playing a crucial role in maintaining the balance between neuronal apoptosis and neurogenesis [16–18]. Previous research has emphasized the role of circadian rhythms and specific core clock genes in regulating stem cell proliferation and differentiation [19]. In mice, the activation of adult neural stem cells is influenced by the circadian cycle, with cell division occurring more frequently during the day and being inhibited by melatonin signals induced by darkness [20]. The core clock gene CRY1 maintains the self-renewal capacity, colony organization and metabolic characteristics of pluripotent stem cells [21]. Disruption of circadian rhythms may compromise the quiescent state of neural stem cells, potentially leading to their premature depletion [22]. This study utilizes ENPCs transgenic reporter mice to investigate the effects of CRD on the differentiation of ENPCs and ENS remodeling, and aims to elucidate the underlying mechanisms.

Methods

Animals

Triple-transgenic mice, Nestin-creER^{T2} × Ngfr-DreER^{T2}: DTRGFP, were generated following our previous protocol [18] to track Nestin^{+}/Ngfr^{+} cells. Briefly speaking, Nestin-creER^{T2} mice were hybridized with R26-e (CAG-RSR-LSL-DTRGFP-WPRE-pA) and Ngfr-e (2 A-DreER^{T2}) mice (purchased from Shanghai Model Organisms Center, Inc). After Tamoxifen (TAM) induction, the newborn Nestin^{+}/Ngfr^{+} cells were labeled with green fluorescent protein (GFP) (Fig. S2A). Specific pathogen-free wild-type male C57BL/6 mice (6–8 weeks old, weight: 20±0.5 g) were purchased from Beijing Vital River

Laboratory Animal Technology Co., Ltd (Beijing, China) and housed in controlled conditions with a standard diet and water ad libitum. Animals were kept in this environment for one week to adapt before experiments. At the end of the experiment, mice were anesthetized with 1.5% isoflurane for euthanasia. All animal studies were authorized by the Animal Care and Use Committee of Union Hospital at Tongji Medical College, Huazhong University of Science and Technology (IACUC No. S2803; approval date: 2021.01.06; approved project: Glutamate regulates gliosis of BMSCs to promote ENS regeneration through α-KG and H3K9/H3K27 demethylation.) and performed in accordance with national guidelines.

Tamoxifen induction

Corn oil was employed as a solvent to dissolve Tamoxifen (TAM) (Sigma-Aldrich) at a concentration of 20 mg/mL, and the resulting solution was stored at 4 °C. For in vivo fate-mapping experiments, Nestin-creER^{T2} × Ngfr-DreER^{T2}: DTRGFP mice were administered 6 intraperitoneal doses of TAM (100 μL) over 6 consecutive days to induce GFP expression in Nestin^{+}/Ngfr^{+} cells [16].

Jet-lagged mice model

As described in a previous study [23], control mice were housed under a strict 12 h light-dark cycle, with lights on at 6 am and off at 6 pm. To induce CRD, mice were subjected to a jet-lag schedule, involving a 6-hour advance of the 12-hour light-dark cycle every 3 days for 8 weeks. To investigate the effect of glial cells on gastrointestinal dysfunction in jet-lagged mice, barium fluorocitrate (FC; 10 mg/kg/day, Sigma-Aldrich) or vehicle (a 1:20 solution of dimethyl sulfoxide (DMSO) and 0.9% NaCl) was administered intraperitoneally every day during the last 4 weeks of the experiment. To investigate the effect of NR1D1/nuclear factor-kappaB (NF-κB) axis on gastrointestinal dysfunction in jet-lagged mice, SR9009 (NR1D1 agonist, 100 mg/kg/day, Selleck) or Bay11-7082 (NF-κB signaling antagonist, 10 mg/kg/day, Selleck) or vehicle (a 1:20 solution of DMSO and 0.9% NaCl) was administered intraperitoneally every 2 days during the last 4 weeks of the experiment.

Gastrointestinal transmission function detection

Mice were fasted overnight but given water before gastrointestinal motility assessment. For whole gut transit time, a carbon black suspension (5% charcoal powder suspended in 10% Arabic gum) was administered orally via gavage, and the time from gavage to the appearance of the first black fecal pellet was recorded. Distal colonic transit time was measured by gently placing a 3 mm metal bead 2 cm proximal to the anal opening using a lubricated plastic Pasteur pipette. The time elapsed from bead placement to expulsion was recorded. Fecal output was determined by collecting total wet feces over a 5 h period. After drying the feces at 100 °C for 2 h, the dry weight was measured. Fecal water content was calculated as [(total wet weight (mg)-dry weight (mg)/ total wet weight (mg)] × 100%. During this process, mice had unrestricted access to food. All gastrointestinal motility experiments were conducted at a fixed Zeitgeber time (ZT 12).

Evaluation of visceral hypersensitivity

Visceral hypersensitivity was assessed using colorectal distension and the abdominal withdrawal reflex (AWR) score. Mice were restrained, and a custom-made catheter with an airbag was gently inserted 1 cm into the anus. The catheter was secured to the tail and connected to a pressure gauge and 20 mL syringe via a three-way adapter. After a 20 min acclimation period in a transparent cage (20 cm × 8 cm × 8 cm), gas was gradually introduced into the airbag, increasing the pressure to 20, 40, 60, and 80 mmHg for 20 s each. A second experimenter recorded the AWR scores, repeating the procedure twice with 5 min intervals. AWR scores were evaluated as previously described [24]. All visceral hypersensitivity experiments were conducted at a fixed Zeitgeber time (ZT 12).

Mice colon tissues collection

Following the completion of in vivo gastrointestinal motility assessments, mice were humanely euthanized at distinct Zeitgeber time (ZT), specifically ZT0, ZT6, ZT12, ZT18, and ZT24. Six mice per experimental group were euthanized at each designated time point. The entire colon was subsequently harvested, with different regions allocated for specific analyses. The proximal colon was collected for Western blot analysis, while the middle section was embedded in paraffin for the preparation of transverse sections. The distal colon was designated for reverse transcription quantitative polymerase chain reaction (RT-qPCR), RNA sequencing, myenteric plexus immunofluorescence analysis, and smooth muscle activity assessment. Colon tissues from five time points (ZT0, ZT6, ZT12, ZT18, and ZT24) were selected for RT-qPCR to examine the expression of clock genes. To ensure temporal consistency with the gastrointestinal function experiments, colon tissues at ZT12 were selected for all other experimental analyses.

Intestinal smooth muscle activity recording

Colon tissues from each group were separated along the mesentery. Luminal contents were then eliminated using Krebs solution (NaCl 118.1 mM/L, KCl 4.8 mM/L, $NaHCO_3$ 25 mM/L, NaH_2PO_4 1.0 mM/L, $MgSO_4$ 1.2 mM/L, glucose 11.1 mM/L, $CaCl_2$ 2.5 mM/L). Afterwards, the mucosa and submucosa were carefully removed, and 8 mm by 2 mm muscle strips were

prepared. Fine silk threads were used to ligate the ends of the muscle strips, which were then floated longitudinally in a tissue bath containing 25 mL of Krebs solution (37 °C, 95% O_2, 5% CO_2). The longitudinal muscle strips were fastened to the isometric force sensor (AD Instruments) and the water bath, and the strips were loaded initially with 1.0 g. The polygraph (LabChart software v.7.0) was used to capture spontaneous smooth muscle activity, and contraction amplitude, frequency, and motility index were all examined after the muscle strips' spontaneous contractions had been stable for 60 min. The tissues were stimulated by electric field stimulation (EFS; 20 V, 500 μs duration, 5 Hz, 5 s) to induce neuronal contraction. Substances capable of modulating neurotransmission pathways, including, atropine (1 μM) and NG-nitro-L-arginine methyl ester (L-NAME, 10 μM) were added to the bath of each organ before EFS to observe the contractile response of the strips.

Immunofluorescence staining

Colonic smooth muscle tissues were isolated to study the morphological alterations of the myenteric plexus. Freshly separated colon tissues were immediately placed in pre-chilled Krebs solution with the mucosal side facing up. Using microforceps, the mucosa and submucosa were carefully removed to expose the muscle layers, which were then treated with 4% paraformaldehyde for 10 min. After washing with phosphate-buffered saline, the tissues were immersed in donkey serum containing 0.3% Triton X-100 for 24 hours to block non-specific binding sites. The samples were then incubated with the primary antibody (Table S1) in 0.3% Triton X-100 at 4°C for 48 hours. Following another wash, the tissues were incubated with the secondary antibody (Table S1) in the dark at 37°C for 2 hours. The nuclei were subsequently stained with 4',6-diamidino-2'-phenylindole dihydrochloride (DAPI) for 10 min. Additionally, tissues were fixed in 4% paraformaldehyde, embedded in paraffin, sectioned, dewaxed, subjected to antigen retrieval, and blocked with serum before being incubated with primary and secondary antibodies (Table S1) to observe the expression of NR1D1 and p65. Finally, confocal microscopy (Nikon, Tokyo, Japan) was used to examine each specimen.

Total protein, cytoplasmic protein and nucleic protein collection

According to the manufacturer's instructions, colon tissues were lysed using using 200 μL radioimmunoprecipitation assay lysis buffer (Beyotime) containing 2 μL of protease inhibitor and 2 μL of phosphatase inhibitor (MedChemExpress) to extract total protein. For the extraction of cytoplasmic and nuclear proteins, the nuclear protein extraction kit (Solarbio) was employed according to the manufacturer's protocol. Protein concentrations were determined using the bicinchoninic acid assay. Proteins were deposited into a 5 × loading buffer and denatured for 15 min at 100 °C. To ensure stability, the proteins were stored at -80 °C.

Western blot

Equal amounts of extracted proteins were subjected to 12.5% sodium dodecyl sulfate-polyacrylamide gel electrophoresis and subsequently transferred to polyvinylidene fluoride membranes. The membranes were blocked with 5% bovine serum albumin at 37 °C for 1 h, followed by an overnight incubation at 4 °C with the primary antibodies (Table S1). GAPDH or β-Tubulin antibodies were used as internal reference controls. After three washes with Tris-buffered saline containing 0.1% Tween 20, the membranes were incubated with goat anti-Rabbit antibody (AntGene) at 37 °C for 1 h. Finally, the blots were visualized and documented using the chemiluminescence imaging equipment (UVP, USA).

RNA sequencing

Total RNA extraction was conducted on distal colonic tissues, and its concentration was quantified using a Nanodrop system (Thermo Scientific). Subsequently, the integrity of the RNA was confirmed through analysis with an Agilent 2100 Bioanalyzer (Agilent Technologies). RNA-seq libraries were meticulously prepared utilizing 2 μg of RNA from each sample, employing the NEBNext mRNA Sample Prep Kit. The resulting libraries underwent sequencing on the BGI-Seq500 sequencing platform and the transcriptome data were supplied by BGI Tech. Differentially expressed genes (DEGs) were ascertained by conducting inter-group gene expression comparisons through DESeq2 version 1.10.1. DEGs were defined based on criteria of |log2 (fold change)| > 1 and a corrected *P*-value less than 0.05. Gene Ontology *Metascape* analysis was conducted utilizing the *Metascape* software [25] (http://metascape.org/gp/index.html), with default settings applied.

RNA isolation and RT-qPCR

The isolation of total RNA from colonic tissues was performed using TRIzol reagent (Vazyme), followed by quantification using a Nanodrop system (Thermo Scientific). For cDNA synthesis, an equal amount of 500 ng RNA was utilized, and cDNA amplification was conducted utilizing a cDNA synthesis kit (Takara Bio) in accordance with the manufacturer's protocol. RT-qPCR was executed using the StepOne Real-Time PCR system (Applied Biosystems) and normalized to GAPDH by applying the △△ Ct method. The primer sequences used in this experiment are provided in Table S2.

Statistical analysis

Statistical analysis of the experimental data was performed using GraphPad Prism v8.0c (GraphPad Software). Results are expressed as mean ± standard deviation. A t-test was used to compare two groups, and one-way analysis of variance (ANOVA) or two-way ANOVA was applied for comparisons among multiple groups. Statistical significance was defined as a *P*-value less than 0.05.

Results

Gastrointestinal motility dysfunction in jet-lagged mice

To investigate the effects of CRD on gastrointestinal motility, we established a jet-lagged mouse model by subjecting mice to an 8-week light/dark phase advance. After 7 weeks of this phase shift, jet-lagged mice exhibited a significantly higher body weight compared to control mice ($P<0.05$, Fig. 1A). Following this, we conducted colorectal distension and assessed AWR scores. The AWR scores for the jet-lagged group at pressures of 20, 40, and 60 mmHg were significantly elevated compared to the control group ($P<0.05$, Fig. 1B), indicating increased visceral sensitivity due to the light/dark phase shift.

Additionally, the jet-lagged mice demonstrated an increase in fecal wet weight ($P<0.01$, Fig. 1C) and fecal water content ($P<0.05$, Fig. 1D), a reduction in whole intestinal transit time ($P<0.01$, Fig. 1E), and a shorter bead expulsion time ($P<0.001$, Fig. 1F) relative to control mice. We further evaluated neuronal contractions induced by electrical field stimulation of colonic muscle strips and assessed the effects of atropine and L-NAME on these contractions. The results revealed that jet-lagged mice exhibited greater contraction tension in response to electrical field stimulation compared to control mice ($P<0.05$, Fig. 1G-H). However, atropine and L-NAME similarly affected contraction tension in both groups ($P>0.05$, Fig. 1G-H). These findings suggest that the enhanced neuronal contractions contributed significantly to the accelerated gastrointestinal motility observed in jet-lagged mice.

Circadian rhythm disruption promoted gastrointestinal motility by increasing enteric glial cell numbers

To investigate the underlying reasons for the enhanced neuronal contractions in jet-lagged mice, we analyzed the changes in neurons and glial cells within the colonic myenteric plexus. Jet-lagged mice exhibited a significant increase in the number of glial cells compared to control mice ($P<0.001$, Fig. 2F), while no significant difference was observed in neuronal cells marked by βIII-Tubulin and HuC/D ($P>0.05$, Fig. 2B-C and F). Further analysis of nitrergic neurons (marked by neuronal nitric oxide synthase, nNOS) revealed a significant increase in these cells in the jet-lagged mice ($P<0.001$, Fig. 2F), whereas the number of cholinergic neurons (marked by choline acetyltransferase, ChAT) remained unchanged ($P>0.05$, Fig. 2F). These findings were corroborated by Western blot analysis, which showed upregulation of GFAP ($P<0.001$) and nNOS ($P<0.01$) protein expression (Fig. 2G-H). Overall, CRD induced structural changes in the myenteric plexus, characterized by an increase in glial cells and nitrergic neurons.

Since L-NAME had comparable effects on EFS-induced muscle contraction intensity in both control and jet-lagged mice, we sought to investigate whether the increased number of glial cells contributed to the enhanced colonic neuronal contractions in jet-lagged mice. To explore this, FC was administered via intraperitoneal injection daily for the final 4 weeks of the jet-lag model. We then assessed visceral sensitivity, and the results showed that FC treatment reduced AWR scores at pressures of 40 and 60 mmHg ($P<0.05$, F-value = 15.81, Fig. S1 A). Additionally, FC treatment decreased fecal output ($P<0.05$, F-value = 9.005, Fig. S1 B) and water content ($P<0.05$, F-value = 4.885, Fig. S1 C), while increasing both whole-gut ($P<0.05$, F-value = 5.417, Fig. S1 D) and colonic transit time in jet-lagged mice ($P<0.05$, F-value = 9.655, Fig. S1 E). FC treatment also reduced the contraction tension of colonic muscle strips in response to electrical field stimulation ($P<0.05$, F-value = 9.395, Fig. S1 F-G). Finally, immunofluorescence analysis confirmed that FC treatment lowered the expression of the glial cell marker GFAP ($P<0.01$, F-value = 39.42) and reduced nNOS ($P<0.05$, F-value = 20.30) expression (Fig. S1 H-I). In summary, CRD enhanced gastrointestinal motility in mice by increasing the number of glial cells.

ENPCs differentiated more into glial cells and nitrergic neurons in jet-lagged mice

Nestin-creER^{T2} × Ngfr-DreER^{T2}: DTRGFP mice were used to track Nestin^{+}/Ngfr^{+} cells. Following a 6-day tamoxifen induction period, adult Nestin-creER^{T2} × Ngfr-DreER^{T2}: DTRGFP mice, characterized by GFP expression correlating with Nestin and Ngfr expression, exhibited GFP-positive cells in the colonic myenteric ganglion. Co-staining was performed with colonic myenteric neuron markers βIII-Tubulin, HuC/D, and nNOS, and the glial cell marker GFAP, alongside GFP. Compared to the control group, the proportion of GFP-positive cells co-expressing GFAP among the total GFAP-positive cells was significantly higher in the jet-lag group (16.55% vs. 23.45%, $P<0.01$, Fig. 3A). Similarly, the proportion of GFP-positive cells co-expressing nNOS among the total nNOS-positive cells was significantly greater in the jet-lag group than in the control group (11.42% vs. 20.17%, $P<0.01$, Fig. 3D). In contrast, there were no significant differences between the control and jet-lag groups

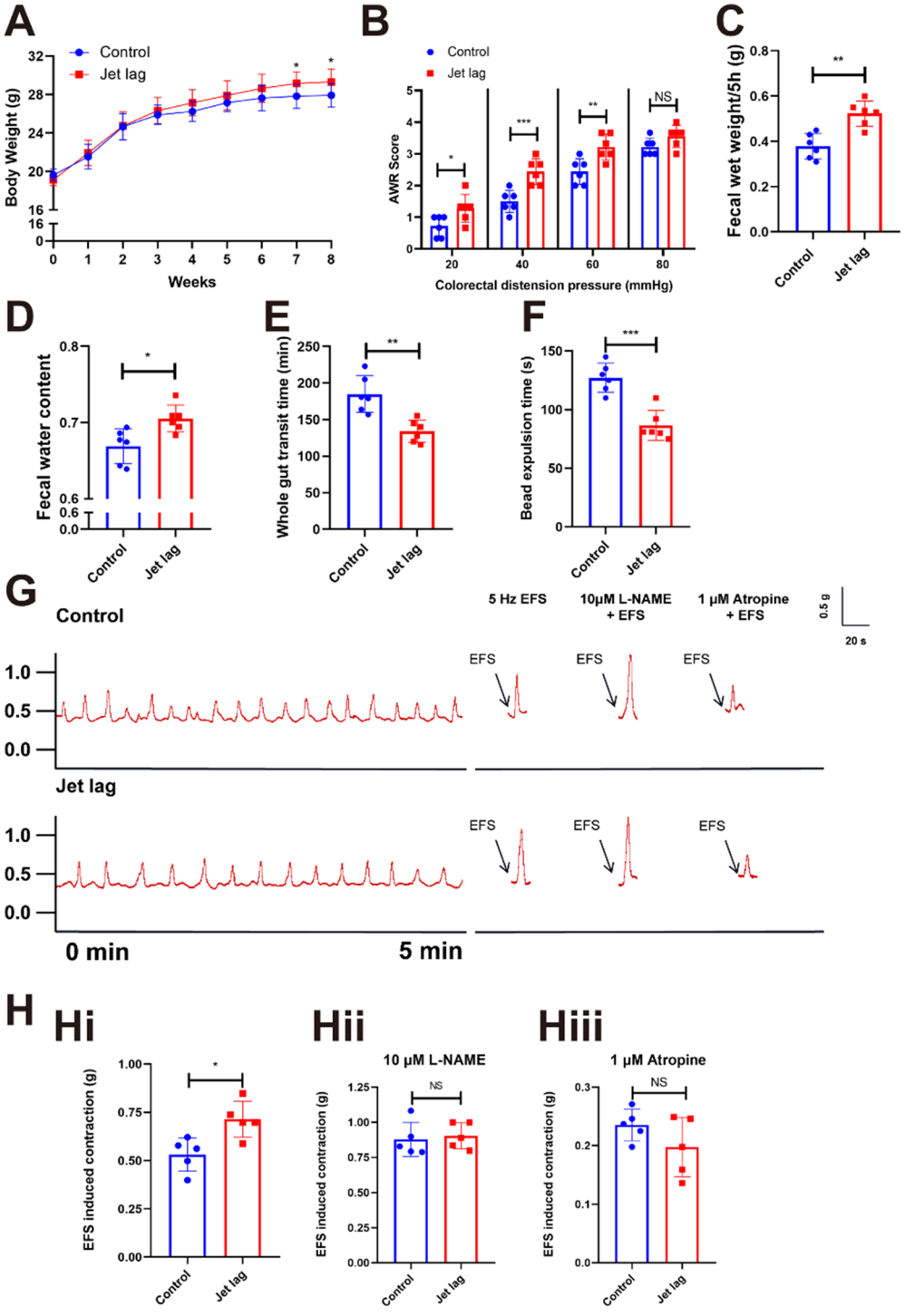

Fig. 1 Jet lag accelerated gastrointestinal motility in mice. (**A**): Body weight changes over time ($n=6$). (**B**). AWR scores at each colorectal distension pressure level ($n=6$). (**C-F**): Effects of jet lag on fecal output, fecal water content, whole gut transit time, and colonic transit time ($n=6$). (**G**): Representative schematic diagram of EFS-induced contraction in colon strips treated with 10 μM L-NAME or 1 μM atropine. (**H**): Quantification of colonic muscle strip contractions in response to EFS across groups ($n=5$). Statistical comparisons between two groups were performed using a t-test. $^{*}P<0.05$, $^{**}P<0.01$, $^{***}P<0.001$. AWR, abdominal withdrawal reflex; L-NAME, NG-nitro-L-arginine methyl ester; EFS, electric field stimulation

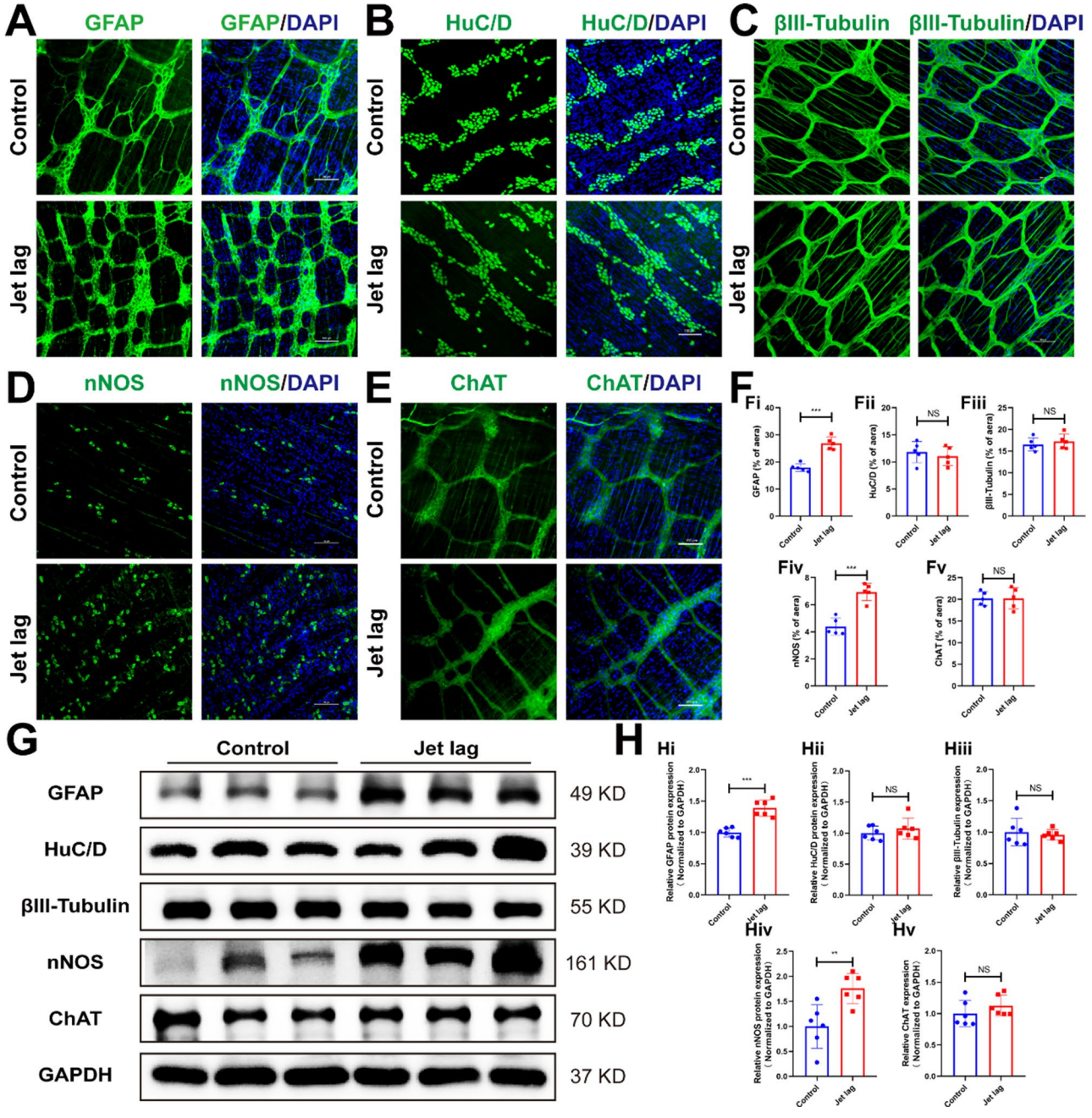

Fig. 2 Jet lag increased glial cells and nitrergic neurons but did not affect enteric neurons. (**A-E**): Representative immunofluorescence confocal laser images of the myenteric plexus in the colon showing markers for GFAP, HuC/D, βIII-Tubulin, nNOS, and ChAT, labeled in green. Nuclei were counterstained with DAPI (blue) (scale bar = 100 μm). (**F**): Quantification of GFAP, HuC/D, βIII-Tubulin, nNOS, and ChAT positive staining in the colon myenteric plexus ($n = 5$). (**G**): Western blot analysis of GFAP, HuC/D, βIII-Tubulin, nNOS, and ChAT protein expression in colon tissue. (**H**): Quantification of the relative protein expression levels of GFAP, HuC/D, βIII-Tubulin, nNOS, and ChAT in the colon tissue across groups ($n = 5$–6). Statistical comparisons between two groups were performed using a t-test. $^{*}P < 0.05$, $^{**}P < 0.01$, $^{***}P < 0.001$

in the proportions of GFP-positive cells co-expressing HuC/D among the total HuC/D-positive cells (4.60% vs. 4.45%, $P > 0.05$, Fig. 3B) or βIII-Tubulin among the total βIII-Tubulin-positive cells (15.20% vs. 15.00%, $P > 0.05$, Fig. 3C). These results suggest that the differentiation of $Nestin^{+}/Ngfr^{+}$ cells into nitrergic neurons and glial cells was significantly increased in the jet-lag group compared to the control group.

Circadian rhythm disruption disturbed NR1D1 gene expression and activated NF-κB signaling in ENPCs

Using RT-qPCR, we carefully examined the relative expression profiles of core clock genes in distal colonic

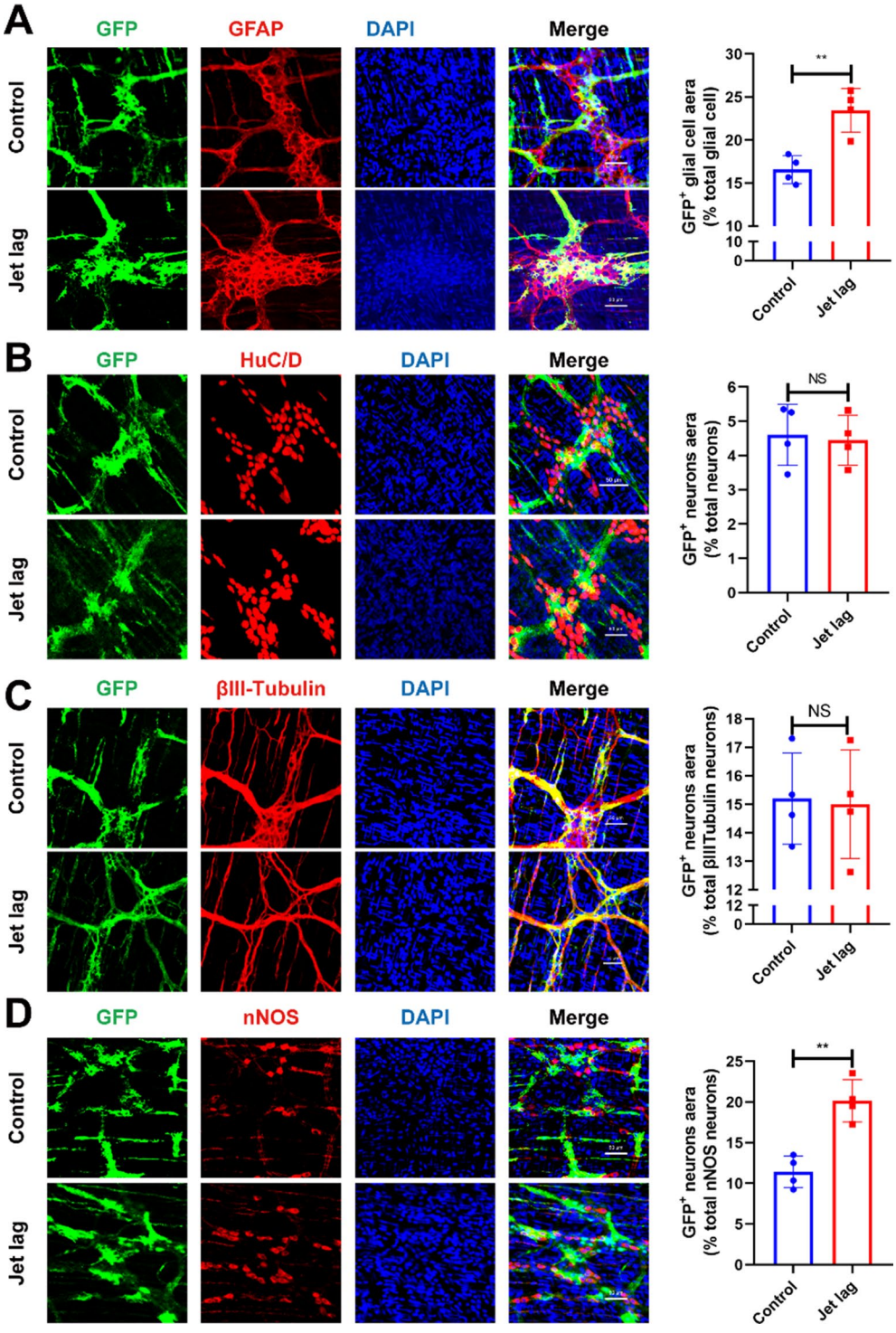

Fig. 3 Effects of jet lag on colonic neurogenesis. (**A-D**): Representative immunofluorescence confocal laser images of freshly prepared intermuscular plexus tissues from the colon, showing GFAP/βIII-Tubulin/HuC/D/nNOS (red) and GFP-labeled ENPCs (green) in both control and jet-lag groups. Nuclei were labeled with DAPI (blue) ($n = 4$, scale bar = 50 μm). Statistical comparisons between two groups were performed using a t-test. $^{*}P < 0.05$, $^{**}P < 0.01$, $^{***}P < 0.001$

tissues at five different time points. A persistent downregulation of *Nr1d1* expression was observed at all time points (Fig. 4A), consistent with the findings from the Western blot analysis ($P<0.01$, Fig. 4C). To further elucidate the molecular mechanisms underlying CRD-induced changes in ENPCs differentiation, we performed whole-genome RNA sequencing to identify differentially expressed genes (DEGs). Gene ontology enrichment analysis of these DEGs revealed significant alterations in distal colonic tissue induced by jet lag. Compared to the control group, the jet-lagged group exhibited a significant enrichment of biological processes related to circadian rhythm and NF-κB signaling (Fig. 4B). Next, we assessed the impact of CRD on NF-κB signaling. CRD significantly enhanced the phosphorylation of IκBα ($P<0.001$, Fig. 4C) and p65 (a subunit of NF-κB) ($P<0.001$, Fig. 4C) in colonic tissues, indicating activation of the NF-κB signaling. Furthermore, an increase in both cytoplasmic ($P<0.01$, Fig. 4D) and nuclear p-p65 ($P<0.01$, Fig. 4D) protein levels in the colonic tissues of jet-lagged mice explained the activation of NF-κB signaling. Consistently, immunofluorescence results showed reduced colocalization of GFP with NR1D1 and increased colocalization of GFP with p65 in ENPCs of the colonic tissue in jet-lagged mice (Fig. 4E-F). In summary, our findings demonstrate downregulation of NR1D1 expression and activation of NF-κB signaling in the ENPCs of colonic tissues in jet-lagged mice.

NR1D1 activation inhibited NF-κB signaling in jet-lagged mice

Previous studies have reported that NR1D1, as a transcriptional repressor, can inhibit the activation of NF-κB signaling [26]. To assess the impact of NR1D1 activation on NF-κB signaling, mice were randomly divided into four groups: control, jet-lag, jet-lag+SR9009, and jet-lag+Bay11-7082. During the final four weeks of the experiment, mice were treated every other day with solvent, SR9009 (NR1D1 agonist), or Bay11-7082 (NF-κB antagonist). Similar to the effects observed with Bay11-7082, SR9009 treatment significantly inhibited CRD-induced phosphorylation of IκBα ($P<0.05$, F-value=19.13) and p65 ($P<0.05$, F-value=7.548) in the colon and reduced the protein levels of cytoplasmic ($P<0.05$, F-value=10.77) and nuclear p-p65 ($P<0.05$, F-value=7.200), indicating that NR1D1 activation suppresses NF-κB signaling (Fig. 5A-B). Consistent with these findings, immunofluorescence analysis showed increased colocalization of GFP with NR1D1 and decreased colocalization with p65 in ENPCs of the colonic tissue in jet-lagged mice after SR9009 treatment (Fig. 5C-D). Collectively, these data suggest that NR1D1 activation inhibited NF-κB signaling in colonic ENPCs.

NR1D1/NF-κB axis ameliorated the ENS in jet-lagged mice

The role of the NR1D1/NF-κB axis in ENPCs differentiation was further investigated. Similar to the effects observed in the jet-lag+Bay11-7082 group (23.63% vs. 18.71%, $P<0.05$, F-value=9.564, Fig. 6A, E), SR9009 treatment significantly reduced the proportion of GFP^+ and $GFAP^+$ double-positive cells among the total $GFAP^+$ cells in jet-lagged mice (23.63% vs. 19.05%, $P<0.05$, F-value=9.564, Fig. 6A, E). Likewise, the proportion of GFP^+ and $nNOS^+$ double-positive cells among the total $nNOS^+$ cells significantly decreased following Bay11-7082 (21.46% vs. 15.15%, $P<0.05$, F-value=11.23, Fig. 6D - E) and SR9009 treatment (21.46% vs. 15.52%, $P<0.05$, F-value=11.23, Fig. 6D - E) in jet-lagged mice. However, SR9009 had no effect on the proportions of GFP^+ and HuC/D^+ double-positive cells among total HuC/D^+ cells (4.93% vs. 5.44%, $P>0.05$, F-value=0.3714, Fig. 6B, E), nor on GFP^+ and $\beta III\text{-}Tubulin^+$ double-positive cells among total $\beta III\text{-}Tubulin^+$ cells (15.24% vs. 14.01%, $P>0.05$, F-value=0.5837, Fig. 6C, E). These findings suggest that SR9009 and Bay11-7082 attenuated the CRD-induced increase in $Nestin^+/Ngfr^+$ cells differentiating into glial cells and nitrergic neurons.

Given the selective impact of the NR1D1/NF-κB axis on CRD-induced ENPCs differentiation, we further examined the effect of NR1D1 activation on neuroanatomical changes within the ENS. Notably, SR9009 and Bay11-7082 treatment had significant effects on the myenteric plexus of the colon (Fig. S2 B). Immunofluorescence analysis revealed that both treatments reduced the number of glial cells (GFAP, $P<0.01$, F-value=27.30, Fig. 6F) and nitrergic neurons ($P<0.001$, F-value=20.30, Fig. 6F), while there were no significant changes in neurons (βIII-Tubulin, HuC/D) among the groups (βIII-Tubulin: $P>0.05$, F-value=0.5256; HuC/D: $P>0.05$, F-value=0.5239, Fig. 6F). Additionally, Western blot analysis corroborated these findings, showing significant downregulation of GFAP ($P<0.05$, F-value=11.23, Fig. 6G-H) and nNOS ($P<0.05$, F-value=18.47, Fig. 6G-H) protein expression after SR9009 treatment, with no significant changes in βIII-Tubulin, HuC/D, or ChAT protein levels (βIII-Tubulin: $P>0.05$, F-value=0.4303; HuC/D: $P>0.05$, F-value=0.2521; ChAT: $P>0.05$, F-value=1.218, Fig. 6G-H). In conclusion, NR1D1 activation remodeled the ENS in jet-lagged mice by inhibiting NF-κB signaling.

NR1D1 activation alleviated gastrointestinal motility dysfunction in jet-lagged mice

Lastly, we investigated the effects of SR9009 and Bay11-7082 treatments on gastrointestinal motility and visceral sensitivity in jet-lagged mice. After two weeks of treatment, both SR9009 and Bay11-7082 slightly reduced the body weight of jet-lagged mice ($P<0.05$,

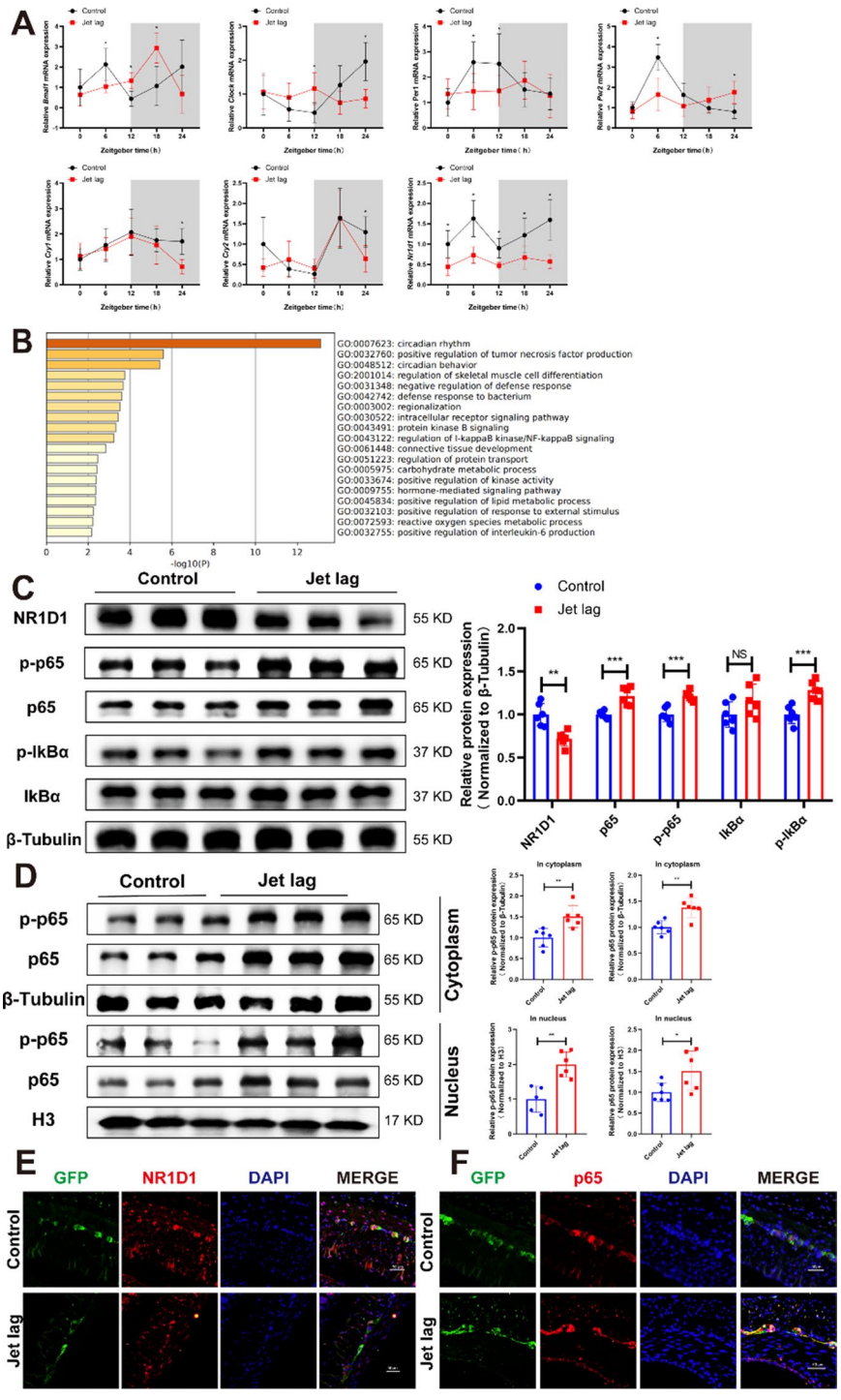

Fig. 4 Jet lag induced NR1D1 downregulation and activated NF-κB signaling in ENPCs of mouse colonic tissues. (**A**): RT-qPCR analysis depicting the relative mRNA expression levels of core clock genes in distal colonic tissues derived from mice exposed to jet lag conditions compared to control mice ($n = 6$). The expression values were normalized to GAPDH mRNA levels. (**B**): The GO enrichment analysis based on *Metascape*. (**C**): Protein expressions of NR1D1, p-p65, p65, p-IκBα, and IκBα in colon tissues measured by Western blot ($n = 5$–6). (**D**): Protein expressions of p-p65, p65, β-Tubulin, and Histone H3 in the cytoplasm (Cyto) or nucleus (Nuc) of colon tissues measured by Western blot ($n = 5$–6). (**E, F**): Representative immunofluorescent images of the colon of NR1D1 (red) and p65 (red) and GFP-labeled Nestin$^+$/Ngfr$^+$ cells (green) in control and jet-lag groups (scale bar = 50 μm). Statistical comparisons between two groups were performed using a t-test. *$P < 0.05$, **$P < 0.01$, ***$P < 0.001$

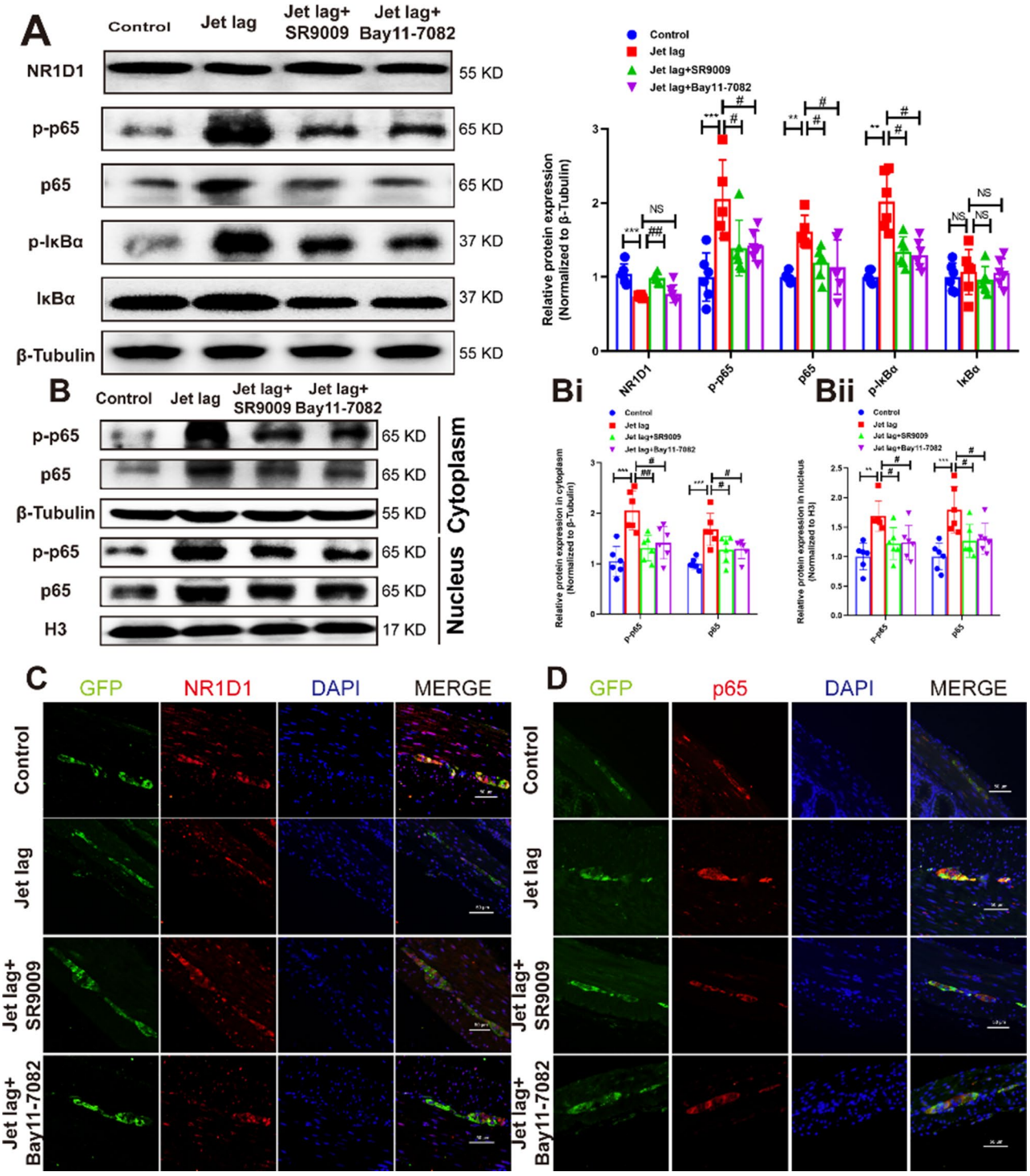

Fig. 5 NR1D1 activation inhibited NF-κB signaling in the colon of mice. (**A**): Western blot analysis of NR1D1, p-p65, p65, p-IκBα, and IκBα in colon tissues ($n = 5–6$). (**B**): Western blot analysis of p-p65, p65, β-Tubulin, and Histone H3 in the cytoplasm (Cyto) or nucleus (Nuc) of colon tissues ($n = 5–6$). (**C, D**): Representative immunofluorescent images of the colon of NR1D1/p65 (red) and GFP-labeled Nestin^{+}/Ngfr^{+} cells (green) in control, jet-lag, jet-lag + SR9009, and jet-lag + Bay11-7082 groups. The nuclei were labeled with DAPI (blue) (scale bar = 50 μm). One-way ANOVA was applied for comparisons among multiple groups. *$P < 0.05$, **$P < 0.01$, ***$P < 0.001$, vs. control; #$P < 0.05$, ## $P < 0.01$, ### $P < 0.001$, vs. jet lag

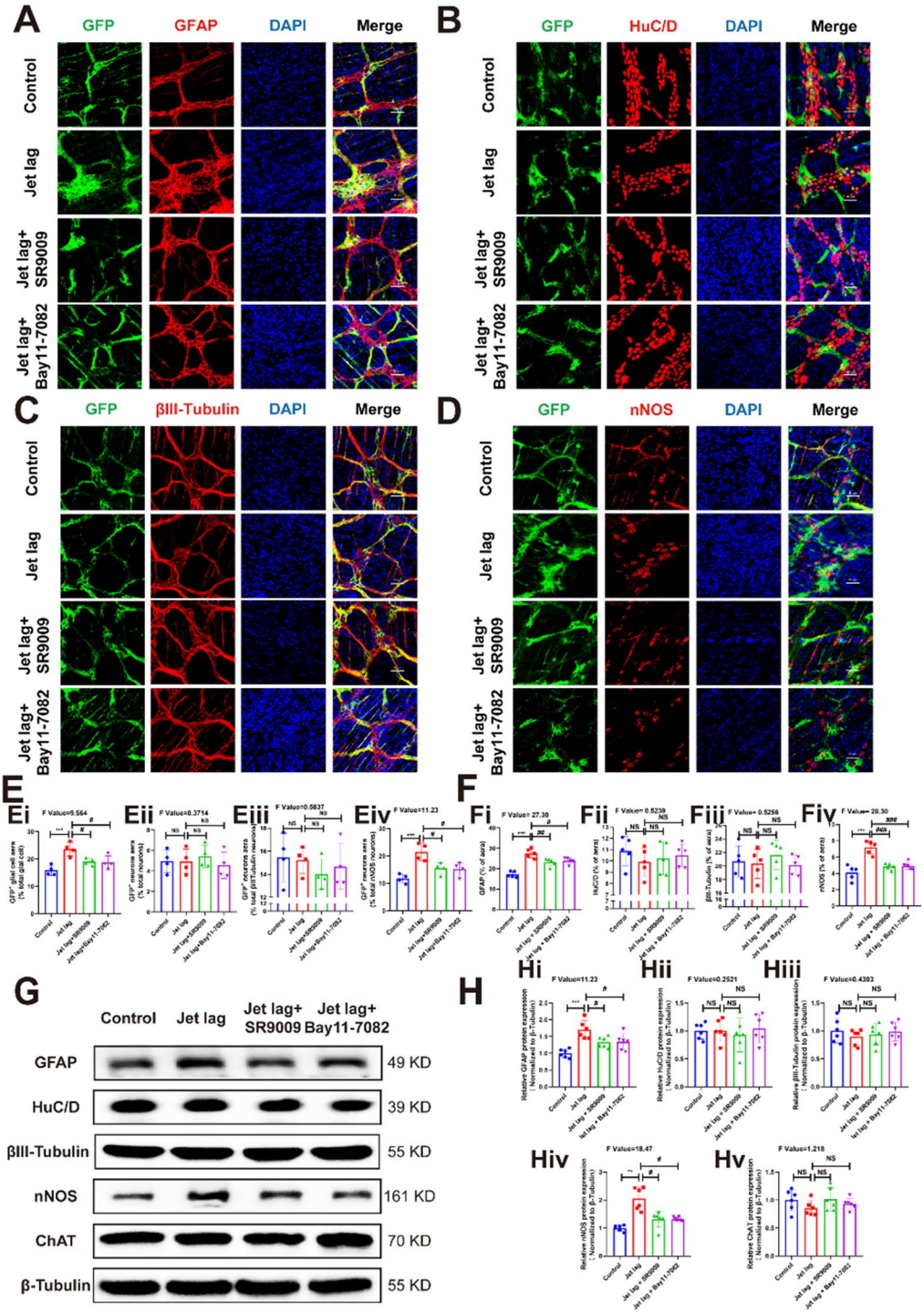

Fig. 6 NR1D1/NF-κB axis ameliorated the ENS in jet-lagged mice. (**A-D**): Representative immunofluorescence confocal laser images in freshly intermuscular plexus tissues of the colon of GFAP/βIII-Tubulin/HuC/D/nNOS (green) and GFP-labeled ENPCs (green) in control, jet-lag, jet-lag + SR9009, and jet-lag + Bay11-7082 groups (scale bar = 50 μm). (**E**): Proportion of ENPCs differentiated into neurons and glial cells ($n = 4$). (**F**): Quantification of GFAP, HuC/D, βIII-Tubulin, and nNOS positive staining in the colon myenteric plexus ($n = 5$). (**G**): Western blot analysis of GFAP, HuC/D, βIII-Tubulin, nNOS, and ChAT protein expression in colon tissue. (**H**): Quantification of the relative protein expression levels of GFAP, HuC/D, βIII-Tubulin, nNOS, and ChAT in the colon tissue across groups ($n = 5$–6). One-way ANOVA was applied for comparisons among multiple groups. $^{*}P < 0.05$, $^{**}P < 0.01$, $^{***}P < 0.001$, vs. control; $\#P < 0.05$, $\#\#P < 0.01$, $\#\#\#P < 0.001$, vs. jet lag

Fig. 7A). SR9009 alone significantly decreased the AWR score at 60 mmHg, suggesting that SR9009 may slightly reduce visceral sensitivity in jet-lagged mice ($P<0.05$, F-value=13.14, Fig. 7B). Both SR9009 and Bay11-7082 treatments significantly reduced fecal pellet output ($P<0.05$, F-value=9.977, Fig. 7C). Additionally, SR9009 treatment decreased fecal water content ($P<0.05$, F-value=7.071, Fig. 7D) and prolonged both whole gut transit time ($P<0.05$, F-value=7.959, Fig. 7E) and colonic transit time ($P<0.05$, F-value=9.236, Fig. 7F). Although Bay11-7082 treatment also showed a mild improvement in gastrointestinal motility in jet-lagged mice, the effect was not statistically significant. These findings suggest that activation of NR1D1 can mitigate the accelerated gastrointestinal motility observed in jet-lagged mice.

Discussion

Circadian rhythms are endogenous oscillations that regulate various physiological and behavioral processes on a 24-hour cycle [27]. Increasing clinical evidence suggests that CRD is a core risk factor for the development and progression of gastrointestinal motility disorders, such as constipation and IBS [7–9]. Despite this, there is limited fundamental research investigating the mechanisms by which CRD induces gastrointestinal motility disorders. In this study, we investigated the impact of CRD on gastrointestinal function in mice and explored its underlying mechanisms. Our results demonstrate that circadian rhythm disruption is associated with symptoms of IBS-D. Specifically, jet-lagged mice exhibited increased visceral sensitivity and accelerated gastrointestinal motility.

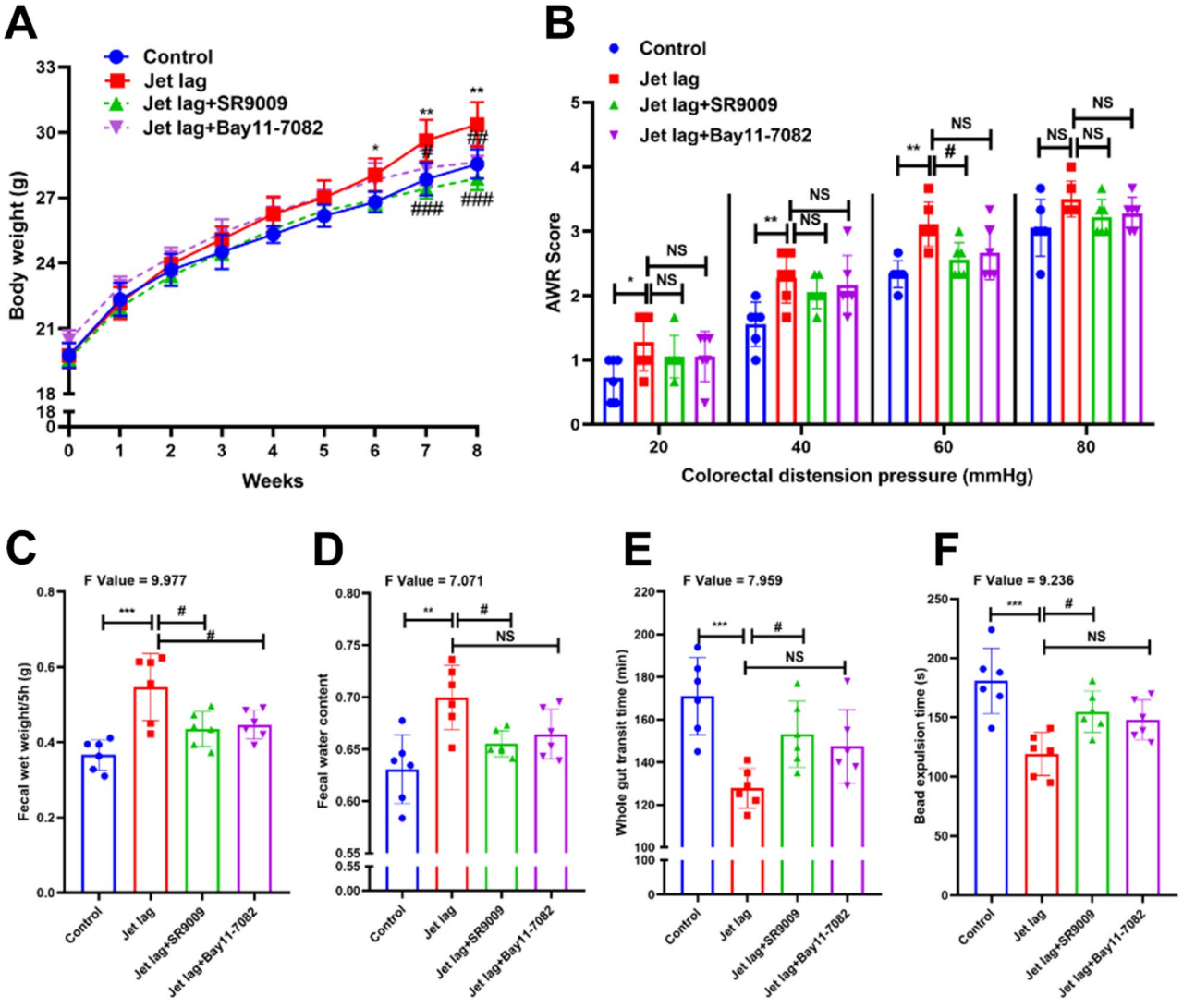

Fig. 7 NR1D1 activation restored gastrointestinal motility in jet-lagged mice. (**A**): Changes in body weight ($n=6$). (**B**): AWR scores at varying colorectal distension pressure levels ($n=6$), two-way ANOVA was applied for comparisons among multiple groups. (**C-F**): Effects of SR9009 and Bay11-7082 on fecal output, fecal water content, whole gut transit time, and colonic transit time ($n=6$). One-way ANOVA was applied for comparisons among multiple groups. *$P<0.05$, **$P<0.01$, ***$P<0.001$, vs. control; #$P<0.05$, ## $P<0.01$, ### $P<0.001$, vs. jet lag. AWR, abdominal withdrawal reflex

Additionally, we observed neuroanatomical changes in the ENS, including an increase in glial cells and nitrergic neurons within the myenteric plexus. Notably, these changes were accompanied by enhanced differentiation of ENPCs into glial cells and nitrergic neurons, potentially mediated by the NR1D1/NF-κB axis.

The ENS is an extensive network comprising intestinal neurons and glial cells, including motor neurons, intrinsic primary afferent neurons, and interneurons. This network plays a crucial role in regulating gastrointestinal motility, secretion, and permeability [12]. One of the most notable features of the ENS is its significant functional and structural plasticity under various conditions of health and disease [10]. Single-cell transcriptomic profiles of the human and mouse ENS indicate circadian rhythm-related expression changes in intestinal neurons [15]. In our study, jet-lagged mice exhibited a IBS-D phenotype, characterized by an increase in the number of glial cells and nitrergic neurons in the colonic myenteric plexus, along with enhanced contraction amplitude in response to EFS. Treatment with glial cell inhibitors fluorocitrate (FC) reduced gastrointestinal transit time, visceral hypersensitivity, and the number of nitrergic neurons in jet-lagged mice. We hypothesize that circadian rhythm disruption may lead to gastrointestinal motility dysfunction by increasing the number of intestinal glial cells. Glial cells display plasticity in their phenotype and can adjust their functions based on cues from the microenvironment to maintain local homeostasis [28]. These cells modulate intestinal neuronal activity through rapid bidirectional communication. Additionally, direct activation of glial cells can drive neurogenic reflexes that control motility and secretion [29, 30]. Thus, the increased glial cells in jet-lagged mice may contribute to gastrointestinal motility disorders by affecting bidirectional communication between neurons and modulating their own activation. Nitrergic neurons are crucial for coordinated peristalsis, and their absence impairs distal relaxation and bolus transport [31], leading to ineffective gastrointestinal propulsion [17, 32]. Previous studies have shown a reduction in nitrergic neurons in transgenic mouse models with glial cell destruction [33]. In our study, FC treatment led to a decrease in nitrergic neurons in jet-lagged mice, suggesting that the increased nitrergic neurons observed in these mice may be a compensatory result of the increased glial cells. Furthermore, we found that while the number of nitrergic neurons increased, the number of cholinergic neurons remained unchanged. It is commonly believed that most myenteric neurons in the adult mammalian ENS are either cholinergic or nitrergic; however, some neurons may express both markers. Additionally, some neurons do not express the rate-limiting enzymes for ChAT or nNOS production [10]. In this study, the observed increase in nitrergic neurons may result from the reprogramming of the existing neuronal population, as well as the generation of new neurons. This research highlights the potential of targeting intestinal glial cells as a promising approach for gastrointestinal diseases and motility disorders.

The enteric nervous system (ENS) is continuously exposed to various external stresses, including mechanical, chemical, and microbial factors, leading to substantial neuronal apoptosis accompanied by equivalent levels of neurogenesis. This dynamic balance helps maintain the overall integrity of the ENS throughout the organism's lifespan [10]. Kulkarni et al. proposed that ENS homeostasis in healthy adult mice is regulated by enteric neural progenitor cells (ENPCs) [16]. Numerous factors influence the regeneration and differentiation of these intestinal stem cells [17]. Our previous research demonstrated that ENPCs can differentiate into neurons and glial lineages within the enteric ganglia, aiding in the repair of ENS in denervated mice [18]. Circadian rhythms play a crucial role in regulating neural stem cell differentiation, neurogenesis, and fate determination [20]. These rhythms can influence adult neural stem cell activation in mice by modulating intracellular calcium dynamics [20]. The coordination between circadian neural circuits and intracellular molecular clocks ensures rhythmic activation of adult neural stem cells. Acute sleep deprivation disrupting circadian rhythms leads to transient overactivation of these stem cells and depletion of the stem cell pool [34]. Consistent with previous studies, our findings reveal the impact of circadian rhythms on ENPCs differentiation. In jet-lagged mice, there is an increased differentiation of ENPCs into glial cells and nitrergic neurons in the colon, while the number of ENPCs differentiating into cholinergic neurons remains unchanged. Supplementation with the core circadian gene NR1D1 agonist reduces the increased differentiation of glial cells and nitrergic neurons in jet-lagged mice. These results underscore the essential role of NR1D1 in regulating ENS homeostasis by modulating ENPCs differentiation.

The whole-genome RNA sequencing and Western blot analyses conducted in this study reveal that NR1D1 expression is downregulated, and NF-κB signaling is activated in the colons of jet-lagged mice. As a transcriptional repressor, NR1D1 inhibits target gene transcription by binding to the corepressor NCoR. Previous studies have demonstrated that NR1D1 can suppress p65 expression by specifically binding to the RevRE element in the p65 promoter region. Activation of NR1D1, in turn, inhibits NF-κB signaling [26]. In mammals, NF-κB exists as dimers composed of five potential Rel/NF-κB family subunits, with the p50 and p65 dimers being the most abundantly expressed in neuronal cells [35]. Consequently, NR1D1 can be regarded as an upstream regulator of p65, inhibiting NF-κB signaling. NF-κB, an inducible

transcription factor present in neurons, glial cells, and neural stem cells, plays a crucial role in maintaining neural stem cell self-renewal and pluripotency. The NF-κB signaling mediated by lymphotoxin β receptors has a dual role in regulating mouse brain neural stem/progenitor cell differentiation, promoting glial lineage differentiation while inhibiting neuronal lineage specification [36]. Notably, NF-κB signaling is indispensable for initiating the differentiation of neural progenitor cells into astrocytic lineages [37]. Guo et al. demonstrated that pharmacological activation of NR1D1 can inhibit LPS-induced microglial activation through NF-κB signaling [38]. In our study, the NR1D1 agonist SR9009 inhibited NF-κB signaling activation in colon ENPCs. Additionally, treatment with the NR1D1 agonist SR9009 and the NF-κB inhibitor Bay11-7082 resulted in reduced differentiation of ENPCs into enteric glial cells and nitrergic neurons in CRD mice. This reduction in enteric glial cells in the colonic plexus improved the dysregulated gastrointestinal motility in jet-lagged mice. Compared to the control group, we observed no change in the number of colonic ENPCs in jet-lagged mice, which is consistent with the observed decrease in neurogenesis and colonic neurons. These findings underscore the critical role of the NR1D1/NF-κB axis in maintaining normal ENS homeostasis in the colon and support the therapeutic potential of NR1D1 agonists for specific diseases.

Conclusions

In conclusion, this investigation elucidates that perturbations in circadian rhythm precipitate the attenuation of NR1D1 expression, consequently triggering the activation of the NF-κB pathway. Subsequently, this molecular cascade culminates in an augmented differentiation of ENPCs into glial cells and nitrergic neurons. Restoration of normal ENPCs differentiation and amelioration of circadian rhythm-disrupted gastrointestinal motility in mice can be achieved through the activation of NR1D1 or inhibition of the NF-κB pathway. This study serves to establish a pivotal foundation for the prospective development of therapeutic interventions targeted at mitigating circadian rhythm-associated gastrointestinal motility disorders.

Supplementary Information

The online version contains supplementary material available at https://doi.org/10.1186/s12967-024-05766-8.

Supplementary Material 1: Fig S1. A. AWR scores at each colorectal distension pressure level ($n=6$), two-way ANOVA was applied for comparisons among multiple groups. B-E: Effects of FC on fecal output, fecal water content, whole gut transit time, and colonic transit time ($n=6$). F: Representative schematic diagram of EFS-induced contraction in colon strips treated with 10 μM L-NAME or 1 μM atropine. G: Quantification of colonic muscle strip contractions in response to EFS across groups ($n=5$). H: Representative confocal laser immunofluorescence images of the colonic myenteric plexus in each group, displaying GFAP, HuC/D, βIII-Tubulin, and nNOS, all labeled in green. Nuclei were counterstained with DAPI (blue) (scale bar = 100 μm). I: Quantification of GFAP, HuC/D, βIII-Tubulin, and nNOS positive staining in the colon myenteric plexus ($n=5$). One-way ANOVA was applied for comparisons among multiple groups. $^{*}P<0.05$, $^{**}P<0.01$, $^{***}P<0.001$, vs. control; #$P<0.05$, ## $P<0.01$, ### $P<0.001$, vs. jet lag. L-NAME, NG-nitro-L-arginine methyl ester; FC, fluorocitrate; EFS, electric field stimulation; AWR, abdominal withdrawal reflex

Supplementary Material 2: Fig S2. A: Immunofluorescence staining showing the co-expression of Nestin (red), Ngfr (gray), and GFP (green), confirming that GFP-positive cells were identified as $Nestin^{+}/Ngfr^{+}$ cells. Cell nuclei were counterstained with DAPI (blue) (scale bar = 50 μm). B: Representative confocal laser immunofluorescence images of the colonic myenteric plexus in each group, displaying GFAP, HuC/D, βIII-Tubulin, and nNOS, all labeled in green. Nuclei were counterstained with DAPI (blue) (scale bar = 100 μm)

Supplementary Material 3: Table S1. The primary and secondary antibodies utilized for western blot analysis and immunofluorescence staining

Supplementary Material 4: Table S2. Primers used for RT-qPCR analysis

Supplementary Material 5

Author contributions

R.L. and H.S. designed and supervised the study. Y.Z. and S.X. contributed equally to this work. Y.Z. and S.X. did the experiment and collected the samples. M.F. and H.Y. did part of the experiment. C.J., and Q.H. interpreted the data and analyses. Y.Z. and S.X. wrote the first draft of the manuscript. All authors contributed to the article and approved the submitted version.

Funding

This work was supported by the National Natural Science Foundation of China (Nos. 82100569, 82300616, 81974068 and 81770539) and the Natural Science Foundation of Hubei Province of China (2023AFB301). The funders had no role in the design of the study, data collection and analysis, interpretation of data, and in writing the manuscript.

Data availability

The datasets used and/or analyzed during the current study are available from the corresponding author on reasonable request.

Declarations

Ethical approval

All animal studies were authorized by the Animal Care and Use Committee of Union Hospital at Tongji Medical College, Huazhong University of Science and Technology. Approval number: IACUC No. S2803; approval date: 2021.01.06; approved project: Glutamate regulates gliosis of BMSCs to promote ENS regeneration through α-KG and H3K9/H3K27 demethylation.

Competing interests

All authors state that they have no conflict of interest.

Received: 27 February 2024 / Accepted: 15 October 2024
Published online: 28 October 2024

References

1. Fagiani F, Di Marino D, Romagnoli A, Travelli C, Voltan D, Di Cesare Mannelli L, Racchi M, Govoni S, Lanni C. Molecular regulations of circadian rhythm and implications for physiology and diseases. Signal Transduct Target Ther. 2022;7(1):41.
2. Guan D, Lazar MA. Interconnections between circadian clocks and metabolism. J Clin Investig 2021, 131(15).
3. Fishbein AB, Knutson KL, Zee PC. Circadian disruption and human health. J Clin Investig 2021, 131(19).
4. Schrader LA, Ronnekleiv-Kelly SM, Hogenesch JB, Bradfield CA, Malecki KM. Circadian disruption, clock genes, and metabolic health. J Clin Investig 2024, 134(14).

5. Bishehsari F, Voigt RM, Keshavarzian A. Circadian rhythms and the gut microbiota: from the metabolic syndrome to cancer. Nat Rev Endocrinol. 2020;16(12):731–9.
6. Salgado-Delgado RC, Espinosa-Tanguma R, Valdés Abadía B, Ramírez-Plascencia OD, Escobar C, Saderi N. Feeding during the resting phase causes gastrointestinal tract dysfunction and desynchronization of metabolic and neuronal rhythms in rats. Neurogastroenterol Motil. 2023;35(12):e14687.
7. Chang WP, Peng YX. Differences between fixed day shift workers and rotating shift workers in gastrointestinal problems: a systematic review and meta-analysis. Ind Health. 2021;59(2):66–77.
8. Nojkov B, Rubenstein JH, Chey WD, Hoogerwerf WA. The impact of rotating shift work on the prevalence of irritable bowel syndrome in nurses. Am J Gastroenterol. 2010;105(4):842–7.
9. Chen HT, Chuang HY, Hsieh TY, Wu PS, Lin FJ, Huang HC, Yang CC, Kuo CH. Shift work is significantly and positively associated with possible gastro-esophageal reflux disease: a meta-analysis study. Front Public Health. 2022;10:980603.
10. Sharkey KA, Mawe GM. The enteric nervous system. Physiol Rev. 2023;103(2):1487–564.
11. Holland AM, Bon-Frauches AC, Keszthelyi D, Melotte V, Boesmans W. The enteric nervous system in gastrointestinal disease etiology. Cell Mol Life Sci. 2021;78(10):4713–33.
12. Spencer NJ, Hu H. Enteric nervous system: sensory transduction, neural circuits and gastrointestinal motility. Nat Rev Gastroenterol Hepatol. 2020;17(6):338–51.
13. Mayer EA, Ryu HJ, Bhatt RR. The neurobiology of irritable bowel syndrome. Mol Psychiatry. 2023;28(4):1451–65.
14. Rieder E, Fernandez-Becker NQ, Sarosiek J, Guillaume A, Azagury DE, Clarke JO. Achalasia: physiology and diagnosis. Ann N Y Acad Sci. 2020;1482(1):85–94.
15. Drokhlyansky E, Smillie CS, Van Wittenberghe N, Ericsson M, Griffin GK, Eraslan G, Dionne D, Cuoco MS, Goder-Reiser MN, Sharova T, et al. The human and mouse enteric nervous system at single-cell resolution. Cell. 2020;182(6):1606–e16221623.
16. Kulkarni S, Micci MA, Leser J, Shin C, Tang SC, Fu YY, Liu L, Li Q, Saha M, Li C, et al. Adult enteric nervous system in health is maintained by a dynamic balance between neuronal apoptosis and neurogenesis. Proc Natl Acad Sci U S A. 2017;114(18):E3709–18.
17. Yarandi SS, Kulkarni S, Saha M, Sylvia KE, Sears CL, Pasricha PJ. Intestinal Bacteria maintain adult enteric nervous system and nitrergic neurons via toll-like receptor 2-induced neurogenesis in mice. Gastroenterology. 2020;159(1):200–e213208.
18. Fan M, Shi H, Yao H, Wang W, Zhang Y, Jiang C, Lin R. BMSCs promote differentiation of enteric neural precursor cells to maintain neuronal homeostasis in mice with enteric nerve Injury. Cell Mol Gastroenterol Hepatol. 2023;15(2):511–31.
19. Benitah SA, Welz PS. Circadian regulation of adult stem cell homeostasis and aging. Cell Stem Cell. 2020;26(6):817–31.
20. Gengatharan A, Malvaut S, Marymonchyk A, Ghareghani M, Snapyan M, Fischer-Sternjak J, Ninkovic J, Götz M, Saghatelyan A. Adult neural stem cell activation in mice is regulated by the day/night cycle and intracellular calcium dynamics. Cell. 2021;184(3):709–e722713.
21. Sato S, Hishida T, Kinouchi K, Hatanaka F, Li Y, Nguyen Q, Chen Y, Wang PH, Kessenbrock K, Li W, et al. The circadian clock CRY1 regulates pluripotent stem cell identity and somatic cell reprogramming. Cell Rep. 2023;42(6):112590.
22. Draijer S, Chaves I, Hoekman MFM. The circadian clock in adult neural stem cell maintenance. Prog Neurobiol. 2019;173:41–53.
23. Thaiss CA, Zeevi D, Levy M, Zilberman-Schapira G, Suez J, Tengeler AC, Abramson L, Katz MN, Korem T, Zmora N, et al. Transkingdom control of microbiota diurnal oscillations promotes metabolic homeostasis. Cell. 2014;159(3):514–29.
24. Jin Y, Ren X, Li G, Li Y, Zhang L, Wang H, Qian W, Hou X. Beneficial effects of Rifaximin in post-infectious irritable bowel syndrome mouse model beyond gut microbiota. J Gastroenterol Hepatol. 2018;33(2):443–52.
25. Zhou Y, Zhou B, Pache L, Chang M, Khodabakhshi AH, Tanaseichuk O, Benner C, Chanda SK. Metascape provides a biologist-oriented resource for the analysis of systems-level datasets. Nat Commun. 2019;10(1):1523.
26. Wang S, Lin Y, Yuan X, Li F, Guo L, Wu B. REV-ERBα integrates colon clock with experimental colitis through regulation of NF-κB/NLRP3 axis. Nat Commun. 2018;9(1):4246.
27. Panda S, Hogenesch JB, Kay SA. Circadian rhythms from flies to human. Nature. 2002;417(6886):329–35.
28. Seguella L, Gulbransen BD. Enteric glial biology, intercellular signalling and roles in gastrointestinal disease. Nat Rev Gastroenterol Hepatol. 2021;18(8):571–87.
29. McClain JL, Fried DE, Gulbransen BD. Agonist-evoked ca(2+) signaling in enteric glia drives neural programs that regulate intestinal motility in mice. Cell Mol Gastroenterol Hepatol. 2015;1(6):631–45.
30. Grubišić V, Gulbransen BD. Enteric glial activity regulates secretomotor function in the mouse colon but does not acutely affect gut permeability. J Physiol. 2017;595(11):3409–24.
31. Mizuta Y, Takahashi T, Owyang C. Nitrergic regulation of colonic transit in rats. Am J Physiol. 1999;277(2):G275–279.
32. Anitha M, Reichardt F, Tabatabavakili S, Nezami BG, Chassaing B, Mwangi S, Vijay-Kumar M, Gewirtz A, Srinivasan S. Intestinal dysbiosis contributes to the delayed gastrointestinal transit in high-fat diet fed mice. Cell Mol Gastroenterol Hepatol. 2016;2(3):328–39.
33. Aubé AC, Cabarrocas J, Bauer J, Philippe D, Aubert P, Doulay F, Liblau R, Galmiche JP, Neunlist M. Changes in enteric neurone phenotype and intestinal functions in a transgenic mouse model of enteric glia disruption. Gut. 2006;55(5):630–7.
34. Liu Q, Luo X, Liang Z, Qin D, Xu M, Wang M, Guo W. Coordination between circadian neural circuit and intracellular molecular clock ensures rhythmic activation of adult neural stem cells. Proc Natl Acad Sci U S A. 2024;121(8):e2318030121.
35. Dresselhaus EC, Meffert MK. Cellular specificity of NF-κB function in the nervous system. Front Immunol. 2019;10:1043.
36. Xiao X, Putatunda R, Zhang Y, Soni PV, Li F, Zhang T, Xin M, Luo JJ, Bethea JR, Cheng Y, et al. Lymphotoxin β receptor-mediated NFκB signaling promotes glial lineage differentiation and inhibits neuronal lineage differentiation in mouse brain neural stem/progenitor cells. J Neuroinflammation. 2018;15(1):49.
37. Birck C, Ginolhac A, Pavlou MAS, Michelucci A, Heuschling P, Grandbarbe L. NF-κB and TNF affect the Astrocytic differentiation from neural stem cells. Cells 2021, 10(4).
38. Guo DK, Zhu Y, Sun HY, Xu XY, Zhang S, Hao ZB, Wang GH, Mu CC, Ren HG. Pharmacological activation of REV-ERBα represses LPS-induced microglial activation through the NF-κB pathway. Acta Pharmacol Sin. 2019;40(1):26–34.

Publisher's note